





Article

Energy and Economic Assessment of a System Integrated by a Biomass Downdraft Gasifier and a Gas Microturbine

Nelson Calderon Henao ^{1,2}, Osvaldo José Venturini ² , York Castillo Santiago ^{3,*} , Electro Eduardo Silva Lora ², Diego Mauricio Yepes Maya ² , Edson de Oliveira Pamplona ², Jhon Steven Navarro Hoyos ¹ and Oswaldo Hideo Ando Junior ^{1,4} 

¹ Research Group on Energy & Energy Sustainability (GPEnSE/CNPq), Federal University of Latin American Integration (UNILA), Av. Sílvia Américo Sasdelli 1842, Foz do Iguaçu 85866-000, PR, Brazil

² Excellence Group in Thermal Power and Distributed Generation (NEST), Federal University of Itajubá (UNIFEI), Av. BPS 1303, Itajubá 37500-903, MG, Brazil

³ Laboratory of Thermal Sciences (LATERMO), Department of Mechanical Engineering (TEM/PGMEC), Fluminense Federal University (UFF), Rua Passo da Pátria 156, Niterói 24210-240, RJ, Brazil

⁴ Cabo de Santo Agostinho Academic Unit (UACSA), Rural Federal University of Pernambuco (UFRPE), Recife 52171-900, PE, Brazil

* Correspondence: yorkcastillo@id.uff.br

Abstract: This work focuses on the energy and economic evaluation of a power generation system composed of a downdraft gasifier and gas microturbine. The gasification process was studied using wood pellets as fuel, while the influence of two gasification agents (air and oxygen-enriched air) on parameters, such as low heating value (LHV), composition, and yield of syngas, were analyzed. The syngas produced from oxygen-enriched air gasification in a downdraft gasifier had an LHV higher than 8 MJ/Nm³, being suitable to be supplied in the gas microturbine. Subsequently, syngas use in the gas microturbine was evaluated, and the results demonstrated that microturbine efficiency dropped from 33.00% to 21.35%, while its power decreased from 200 kW to 81.35 kW. The power generation system was modeled using Aspen Plus[®] v 11.0 software and validated using results obtained from published experimental studies. Accordingly, the integrated generation system presented an overall efficiency of 11.82% for oxygen-enriched air gasification cases. On the other hand, an economic assessment through risk analysis using Monte Carlo simulations was performed using Crystal Ball[®] v11.1.2.4.850 software. The economic results indicated that the implementation of a generation system was economically unfeasible, however, if the electricity rate price was increased by 63%, the proposed configuration could be feasible.

Keywords: downdraft gasifier; gas microturbine; syngas; economic assessment; Monte Carlo evaluation



Citation: Calderon Henao, N.; Venturini, O.J.; Castillo Santiago, Y.; Silva Lora, E.E.; Yepes Maya, D.M.; Pamplona, E.d.O.; Navarro Hoyos, J.S.; Ando Junior, O.H. Energy and Economic Assessment of a System Integrated by a Biomass Downdraft Gasifier and a Gas Microturbine. *Processes* **2022**, *10*, 2377. <https://doi.org/10.3390/pr10112377>

Academic Editors: Francesca Raganati and Denny K. S. Ng

Received: 6 October 2022

Accepted: 10 November 2022

Published: 12 November 2022

Publisher's Note: MDPI stays neutral with regard to jurisdictional claims in published maps and institutional affiliations.



Copyright: © 2022 by the authors. Licensee MDPI, Basel, Switzerland. This article is an open access article distributed under the terms and conditions of the Creative Commons Attribution (CC BY) license (<https://creativecommons.org/licenses/by/4.0/>).

1. Introduction

The world energy scenario presents a progressive growth in demand due to economic and population expansion, which implies a substantial increase in fossil fuel consumption that harms the environment and compromises the quality of life of current and future generations [1]. In order to face global challenges in energy security, climate change, and economic growth, it is necessary to develop low-carbon technologies that can be powered with biofuels and meet future energy requirements, especially those of communities away from large urban areas centers [2].

Among these technologies, one could highlight the gas microturbine. In this prime mover, atmospheric air is suctioned by a centrifugal compressor, and prior to entering the compressor, it passes through the gaps between the electric generator's stator and the arrangement's housing. After leaving the compressor, the air is directed through the regenerator, a heat exchanger that preheats the air (oxidant); then, the preheated air is directed to the combustion chamber, where fuel is injected and burnt. After the combustion

reaction, the hot gases circulate through a radial turbine rotor, promoting the shaft's rotation and simultaneously driving the compressor and the electric generator. Once the flue gases leave the turbine rotor, they are led through the regenerator and released into the atmosphere [3]. The microturbine's structural configuration may change with the manufacturer and application, but generally, it operates in a single-shaft arrangement with a regeneration system. Non-regenerative gas microturbines have an average efficiency of around 17%, while regenerative microturbines can reach efficiencies of up to 35% [4].

Similar to traditional gas turbines, the temperatures that the microturbines' construction materials can withstand limit the possibilities for their range of operation. In this sense, the microturbine combustion chamber is fed with a high air-fuel ratio to obtain low-temperature combustion gases, reducing thermal NO_x emissions [5]. The residence period of the fuel-air mixture inside the microturbine combustion chamber is enough to promote complete combustion, as well as reduce CO content and unburned hydrocarbon emissions [6]. Thanks to the synergy between power control and combustion systems, gas microturbines can be fed with various fuels. In general, different fuels can be used without significant changes to system components; residual heat from exhaust gases, even after the regeneration process, can be used in cogeneration applications, such as water heating or low-pressure steam generation [7].

The main operational concerns of gas microturbines are associated with damage to components subjected to high temperatures and their susceptibility to severe degradation when there are excess contaminants in the fuel and air supplies. Droplets found in gaseous fuels can also cause structural damage to the microturbine [8]. A concerning phenomenon when burning fuels of low energetic densities is the possibility of compressor surging. This phenomenon manifests as a return of the working fluid from the combustion chamber towards the compressor exit due to the necessity of reducing the airflow fed in the combustion chamber (a lower volume of oxidizer is required during the oxidation of the gas), which leads to an increase in compressor pressure ratio. Notably, concerns with the combustion and fuel injection systems vastly outweigh the engine's mechanical problems [9].

On the other hand, the gasification process consists of converting solid or liquid fuels into a fuel gas (called syngas), enabling its use in prime movers, such as internal combustion engines, gas turbines, and microturbines, aiming for power generation [10]. Syngas is the name given to a mixture of hydrogen, carbon monoxide, and methane that can be produced from natural gas, coal, oil, biomass, and even from organic waste. Syngas represents a potentially growing source of clean fuels and also for the synthesis of chemical products [11]. The gasification process needs a gasifying medium, also called a gasification agent, which allows the rearrangement of the molecular structure of the raw material; steam, oxygen, air, carbon dioxide, hydrogen, or a mixture of them are typically used as gasification agents [12]. The gasification agent reacts with solid carbon and the heavier hydrocarbon content of fuels, transforming them into low molecular weight gases, such as CO, CH₄, and H₂ [11].

It is worth noting that when the gasification process is carried out with air, the syngas has a considerable content of nitrogen, which reduces the heating value of syngas (4–6 MJ/Nm³), decreasing the general efficiency of gasification plants [13]. Syngas with an average calorific value of 5.0 MJ/Nm³ can be used directly in combustion engines or for direct burning in furnaces and boilers [14]. One solution for the dilution effect of nitrogen is to use oxygen-enriched air as a gasification agent. The use of oxygen-enriched air raises the syngas calorific value since a lower nitrogen content in the gasification agent leads to a higher concentration of combustible gases in the producer gas, such as hydrogen and carbon monoxide [15]. It also improves the process temperature and reaction rate, and meanwhile the volume of produced flue gas and tar content decreases [16].

Usually, oxygen-enriched air could be obtained through cryogenic distillation, pressure swing adsorption, and membrane-based separation. Cryogenic distillation and pressure swing adsorption have the advantage of producing oxygen with high purity (higher than 99.5 vol%); however, for these processes there are high energy requirements to sustain

high compression ratios and low operating temperatures [17]. The membrane-based separation process (considered in this study) is an attractive alternative for oxygen-enriched air production with O₂ purity in the range of 40–50% due to its lower cost than other technologies, rendering the process suitable for biomass thermochemical conversion [18].

Recently, several authors have developed gasification models and compared the use of air and oxygen-enriched air as gasification agents. Sittisun et al. [19] evaluated two biomasses (corn cobs and corn stover) as feedstocks for syngas production in a downdraft gasifier. Cao et al. [20] compared the effect of temperature, ER, and oxygen enrichment on syngas yield and LHV using five biomasses (pine sawdust, rice husk, corn core, legume straw, and wood chips) through Aspen Plus software. Gu et al. [21] analyzed the effects of the operating conditions of rice straw gasification on energy/exergy efficiencies, LHV, and syngas composition. The authors found that the gasification efficiency and syngas quality obtained with oxygen-enriched air were higher than those obtained with air. However, these studies did not explore syngas use in prime movers or in integrated systems for electricity generation.

Several authors have been working on solutions combining gas microturbines with gasifiers for the efficiency and reliability of the generation systems. In the case of coupling microturbines to syngas production technologies, it is necessary to increase the fuel flow and pressure to guarantee that the combustion chamber will supply adequate thermal energy [22]. Rabou et al. [23] evaluated the performance of a gas microturbine using mixtures of syngas with natural gas. For the low energy density gas (syngas) application in the microturbine, the study showed that the maximum fuel gas flow allowed by the fuel control unit limited the achievable power. With a partial load operation, the lower limit for stable microturbine operation was 8 MJ/Nm³ for low heating value (LHV) syngas.

Page et al. [24] analyzed the relationship between syngas composition and flashback and blowout propensity for a gas microturbine with a rated power of 60 kW and concluded that, for a hydrogen content of less than 30%, flame instability was not observed. Moradi et al. [25] studied a small combined heat and power system composed of a fluidized bed gasifier, a 100 kW gas microturbine, and an organic Rankine cycle unit. The results showed that the integrated system produced 127.6 kW of electricity and 78.7 kW of useful heat, with an electrical efficiency of 23.6%. The inclusion of the gas microturbine brings the environmental benefits of reducing emissions of nitrogen oxides (NO_x) and carbon monoxide (CO). However, other implications must be considered, such as the additional costs of system maintenance.

Perna et al. [26] evaluated the performance of a small-scale hybrid plant composed of a gas microturbine and a solid oxide fuel cell (SOFC). The hybrid plant was fed with syngas produced in a downdraft gasifier, obtaining 262 kW of electrical energy (SOFC provided 180 kW) and 405 kW of thermal energy, while the electrical and cogeneration efficiencies were 35% and 88%, respectively. Renzi et al. [27] simulated a 100 kW gas microturbine fed with syngas and natural gas, verifying that the injection of steam increases the power produced by the microturbine in both cases. Regarding emissions, the authors observed that NO_x could be reduced by up to 75%, while CO concentration increased slightly when syngas was used. Corrêa et al. [28] studied the effect of using syngas and natural gas mixtures in a 30 kW microturbine. The evaluation focused on turbine performance features, which include turbine efficiency, outlet temperature, and air/fuel flow rate. Tests performed with the microturbine showed that efficiency dropped (26.0% to 22.7%) when the fuel was replaced from pure natural gas to a mixture of natural gas and syngas (50%/50%). This drop in the gas microturbine efficiency is associated with syngas use because, as it is a low energy density fuel, the injection system must provide a higher flow rate than the nominal flow rate for the reference fuel (natural gas). Thus, it is necessary to increase the diameter of the pipes and valves, as well as redesign the spiral flame of the chamber to optimize combustion, and for this study, these structural modifications were not considered. Furthermore, the temperature analysis for different experimental conditions showed little variations in the

output temperature of the microturbine (3 °C maximum increase in temperature), despite the change in the fuel composition.

Therefore, this paper aims to analyze biomass gasification as an alternative for managing wastes produced, with the simultaneous generation of by-products, such as electricity. Thus, this proposal seeks to contribute to developing a new system that combines a gasifier, air separation unit, and gas microturbine to generate electricity with low emissions and a high potential for implementation in regions away from large urban centers considering the Brazilian scenario. For this purpose, employing Aspen Plus™ software, the biomass waste gasification process using air and oxygen-enriched air was modeled. After validating the gasification model, different parameters, such as cold gas efficiency, composition, yield, and syngas LHV, were assessed. Subsequently, using the model developed in Aspen Plus™, an analysis of using syngas in microturbines was performed to determine the potential of electricity generation via the integrated downdraft gasifier/microturbine system. The behavior of the technologies operating together is characterized in detail through sensitivity analysis, in terms of both overall thermal performance and engine efficiency. Finally, the main parameters that determine the economic feasibility of a generation system, such as the one proposed here, are assessed, and their applicability in the Brazilian context is analyzed. Additionally, this work provides support for a better understanding of the process of technical and economic evaluation of the thermochemical conversion of biomass into syngas and its potential use for electricity generation.

2. Materials and Methods

This research was developed considering the research methodology presented in Figure 1. The proposed system was modeled and analyzed using AspenPlus® v 11.0 software (Aspen Technology Inc; Bedford, MA, USA), while the economic assessment was performed in Crystal Ball® v11.1.2.4.850 software (Oracle Corporation; Austin, TX, USA). Different operating conditions of gasification processes were investigated to determine the optimum operating points of the proposed system. All the results were validated using experimental and computational data from specialized literature.

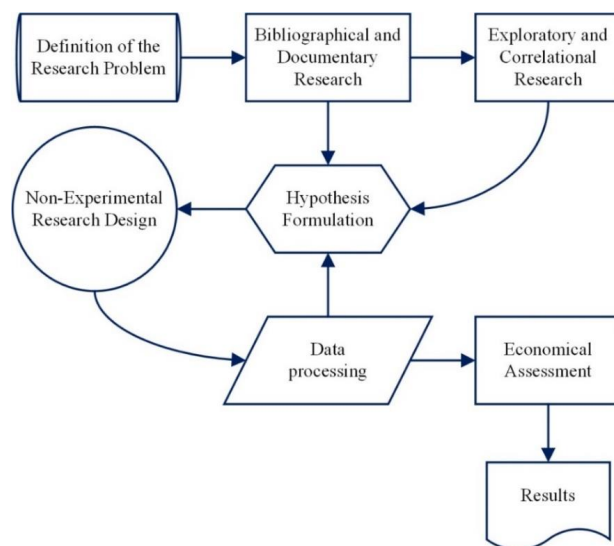


Figure 1. Methodology scheme.

2.1. Downdraft Gasifier Model

The Peng–Robinson method with Boston–Mathias modifications was used to estimate the variation of the thermodynamic state of the different processes that coexist inside the downdraft gasifier. This method is recommended for establishing the thermodynamic state of non-polar and moderately polar substances, such as non-petroleum hydrocarbons. The

standard of the International Association for the Properties of Water and Steam (IAPWS-95) was implemented to calculate the thermodynamic properties of the free water phase of the system, considering a solubility factor of 3.

The enthalpy and density properties of the unconventional compounds were parameterized using the HCOALGEN and DCOALIGT methods, respectively. The HCOALGEN method is based on empirical correlations to estimate the enthalpy of combustion, the enthalpy of formation, and the specific heat of the compound; the DCOALIGT method is based on empirical correlations from the Institute of Gas Technology to determine the density of the compound.

Wood pellets were considered as fuel for the gasification process. The ultimate and proximate analyses are presented in Table 1.

Table 1. Ultimate and proximate analysis of fuel used [29].

Ultimate Analysis		Proximate Analysis	
Component	Content [%]	Component	Content [%]
Carbon	50.70	Volatiles (Dry Basis)	85.40
Hydrogen	5.90	Fixed Carbon (Dry Basis)	14.40
Oxygen	43.00	Ash (Dry Basis)	0.20
Nitrogen	0.19	Moisture (Wet Basis)	7.20
Sulfur	5×10^{-3}		
Chlorine	5×10^{-3}		
Ash	0.20		

The scheme of the downdraft gasifier model developed in Aspen Plus® software is presented in Figure 2. In steady state operation, the pretreated biomass stream (BIOMASS) enters the pyrolysis zone (PYROZON) of the gasifier; at this stage, the biomass devolatilization is supported by the heat flux (Q0) from the combustion zone (COMBUZON). The pyrolysis product (DECOMP) contains chemical species in the solid and gaseous phase, which are sent to the gasifier combustion zone (COMBUZON), where the exothermic reaction occurs, releasing chemical energy for all zones.

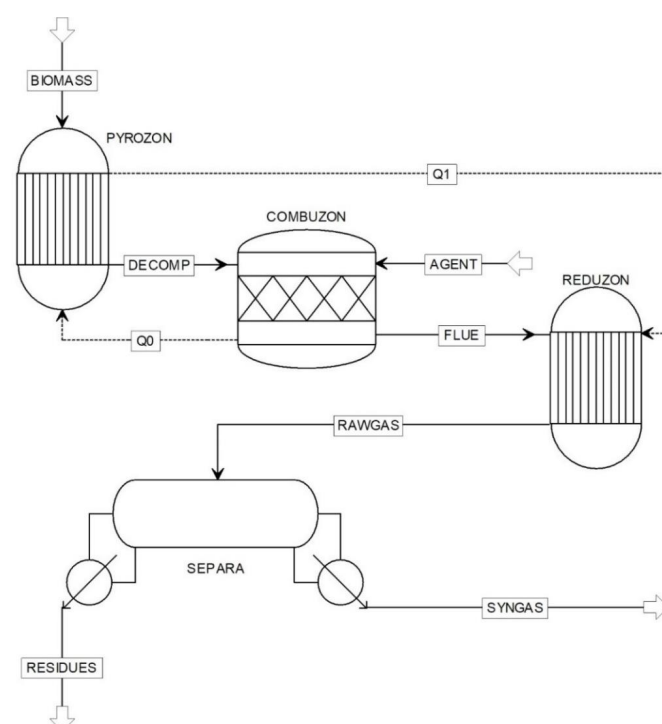


Figure 2. Downdraft Gasifier Model.

These reactions (Table 2) are possible due to feeding a gasification agent (AGENT), which is essential to promote the oxidation reactions. The combustion gases (FLUE) are directed to the reduction zone (REDUZON), where the chemical reactions responsible for the gross syngas production (RAWGAS) occur.

Table 2. Reactions in the gasification process.

Code	Chemical Reaction	Reaction Name	Reaction Heat (kJ/mol)	Zone
R1	Biomass \rightarrow volatiles + char	Biomass pyrolysis	-	PYZON
R2	$\text{H}_2 + 1/2\text{O}_2 \rightarrow \text{H}_2\text{O}$	Hydrogen oxidation	-242	COMBUZON
R3	$\text{CO} + 1/2\text{O}_2 \rightarrow \text{CO}_2$	Monoxide carbon oxidation	-238	COMBUZON
R4	$\text{C} + 1/2\text{O}_2 \rightarrow \text{CO}$	Partial oxidation of char	-111	COMBUZON
R5	$\text{C} + \text{O}_2 \rightarrow \text{CO}_2$	Total oxidation of char	-394	COMBUZON
R6	$\text{C} + \text{CO}_2 \rightleftharpoons 2\text{CO}$	Boudouard reaction	+172	REDUZON
R7	$\text{CO} + \text{H}_2\text{O} \rightleftharpoons \text{CO}_2 + \text{H}_2$	Shift reaction	-41	REDUZON
R8	$\text{C} + \text{H}_2\text{O} \rightleftharpoons \text{CO} + \text{H}_2$	Char gasification	+131	REDUZON
R9	$\text{C} + 2\text{H}_2 \rightleftharpoons \text{CH}_4$	Char hydrogenation	-75	REDUZON
R10	$\text{CH}_4 + \text{H}_2\text{O} \rightleftharpoons \text{CO} + 3\text{H}_2$	Steam methane reforming	+206	REDUZON

It is worth noting that the thermal energy required for the endothermic reactions of PYROZON is supplied by the COMBUZON (exothermic reactions), while the thermal requirements for the endothermic reactions in the REDUZON are met through the heat released in the COMBUZON, which is partially used in the PYROZON or through the thermal energy released by the shift reaction (exothermic reaction). The RAWGAS still needs to be cleaned and dried; this process is represented by a separator (SEPARA) that delivers both the final clean syngas (SYNGAS) and some residues (such as soot, moisture, and ash).

The model was developed considering the Gibbs's free energy minimization method, where the maximum possible energy conversion can be obtained at a thermodynamic equilibrium state. Equation (1) can determine the syngas composition at different operational conditions.

$$G^t = \sum_{i=1}^N n_i \Delta \bar{G}_{f,i}^\circ + \sum_{i=1}^N n_i RT \ln \left(\frac{n_i}{n_{tot}} \right) \quad (1)$$

where $\Delta \bar{G}_{f,i}^\circ$ corresponds to the standard Gibbs free energy of formation for each specie, n_i is the molar number of each specie, n_{tot} is the total molar amount, and R and T represent the ideal gas constant and system temperature, respectively.

The baseline study was created using only atmospheric air as a gasification agent and an equivalence ratio (ER) of 0.30, as suggested by Basu [30]. The stoichiometric amount of air required to complete biomass combustion was determined by an independent simulation within AspenPlus® itself. This simulator consisted of a calculator block, which determined the empirical formula of the biomass considering its ultimate analysis and later calculated the stoichiometric coefficients of the other chemical compounds present in the combustion reaction. Finally, the stoichiometric air/fuel ratio was calculated, which is useful for variations in the equivalence ratio. Thus, it was calculated that one kilogram of wood pellets requires approximately 5.537 kg of atmospheric air (or 1.29 kg of oxygen) to achieve stoichiometric combustion. In the scenario that considers pure atmospheric air as a gasification agent, the oxidant deficit flow was entered into the downdraft gasifier through Equation (2).

$$\text{AIR} = \text{ER} \times 5.537 \times \text{BIOMASS} \quad (2)$$

where AIR is the airflow amount (kg/h) supplied in the combustion zone and BIOMASS is the mass flow of fuel fed in the pyrolysis zone (kg/h).

For the scenario that uses oxygen-enriched air as a gasification agent, it was necessary to introduce a minor modification in the downdraft gasifier model originally presented in Figure 2. In this sense, an air separation unit (ASU) based on polymeric membranes

technology (Figure S1 on Supplementary Materials) was introduced in the model. Despite having relatively low separation yields (up to 50% oxygen content), this technology is low-cost and has low-energy consumption [31]. The composition of the atmospheric air, the concentrations of the oxygen-enriched gasification agent flow, and nitrogen fractions removed from atmospheric air, for an ER = 0.30, are shown in Table 3.

Table 3. Oxygen concentration in AGENT flow and nitrogen fractions removed in ASU block.

Oxygen Volumetric Concentration in AGENT Flow [%]	Nitrogen Volumetric Concentration in AGENT Flow [%]	Removed Nitrogen Flow [kg/h]	Removed Nitrogen Split Fraction at ASU Block [-]
21	79	0	0
25	75	25.26	0.2025
30	70	47.37	0.3797
35	65	63.16	0.5063
40	60	75.01	0.6013

2.2. Validation of Gasification Model

Considering the need to validate the proposed gasification model, it was necessary to expand and adapt the present model for the thermochemical conversion of different biomasses. Once the simulation modeling in Aspen Plus[®] was adapted, a comparative analysis was carried out between the main results obtained through the simulation model proposed in this study and the results reported by some bibliographic references, using air as a gasifying agent and a pressure around 1 bar.

Table 4 presents the gasifier operating conditions and the type of raw material to be gasified. For the validation, the main parameters of the gasification performance compared correspond to syngas volumetric composition in terms of CO, CO₂, H₂, and CH₄, as well as syngas LHV and gasification temperature.

Table 4. Validation of the downdraft gasifier model results.

Parameter	Units	Values			
Average gasification zone temperature	°C	850	850	800	800
Equivalence ratio	[-]	0.36	0.36	0.27	0.27
Biomass	N/A	Wood chip	Wood Chip	Wood Pellets	Wood Pellets
Low heating value	MJ/Nm ³	4.85	4.70	5.14	5.52
Composition					
H ₂	%	15.23	16.39	18.32	21.37
CO	%	23.04	20.91	20.93	19.29
CO ₂	%	16.42	17.16	12.87	11.72
CH ₄	%	1.58	0.8	3.09	2.2
N ₂	%	42.31	44.54	44.79	45.42
Other species	%	1.42	0.2	-	-
Source	N/A	[32]	This model	[33]	This model
RMS	N/A	-	1.49	-	1.55

The deviation between model results and the experimental data was calculated using the root-mean-square (RMS) error, shown in Equation (3).

$$RMS = \sqrt{\frac{\sum_i (exp_i - sim_i)^2}{N}} \quad (3)$$

where exp_i are the experimental data from the literature [32,33], sim_i are the values from the gasification model, and N is the number of measures.

2.3. Gas Microturbine Model

The gas microturbine model developed in this study considers the parameters of the Capstone C200 microturbine produced by Capstone Green Energy (Los Angeles, CA, USA) with a nominal power of 200 kW. The microturbine operating principle is based on the Brayton regenerative cycle, as shown in Figure 3.

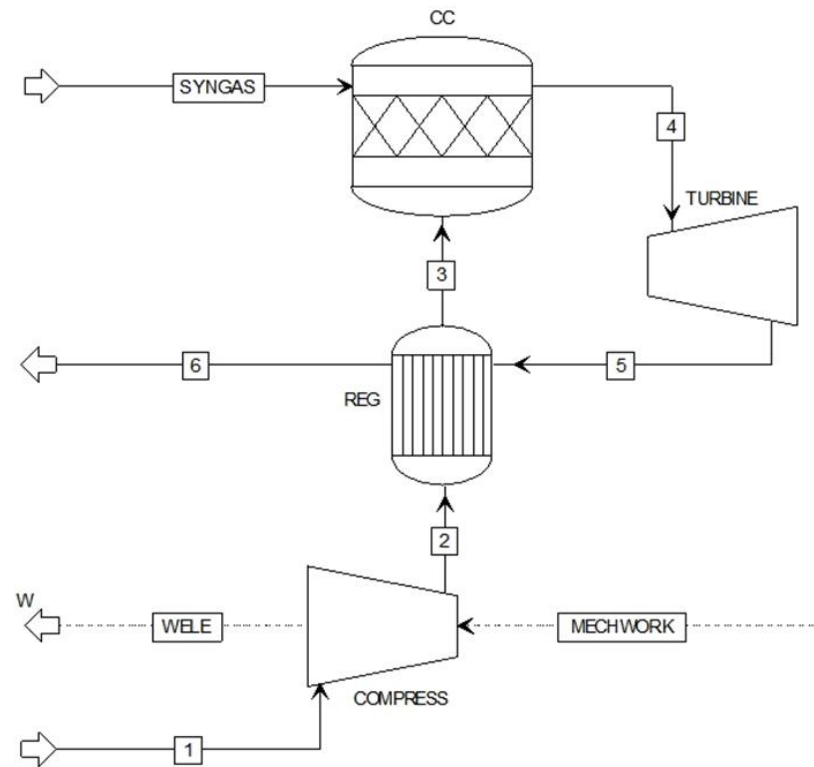


Figure 3. Gas microturbine scheme.

The microturbine cycle is described as follows: the airflow (flow 1) enters the compressor (COMPRESS), then the compressed air (flow 2) circulates through the regenerator (REG) and is later transferred to the combustion chamber (CC), where it will be mixed with the fuel (SYNGAS) that enters the combustion chamber. The resulting combustion gases (flow 4) are directed to the TURBINE, where expansion and mechanical work are generated. The expanded gases (flow 5) pass through REG before being released into the atmosphere. A fraction of the mechanical work obtained during the expansion in the turbine is used to drive the compressor; the rest of the mechanical work is transferred to the electrical generator and converted into electricity.

Based on the syngas LHV, the required fuel flow was recalculated without exceeding the maximum limit stated by the manufacturer, i.e., without requiring structural changes to the engine combustion system.

The airflow supplied into the combustion chamber must be controlled, aiming for the oxygen fraction of combustion gases (flow 4) not to exceed 15% [34]. Thus, it was necessary to implement Equation (4) within the model to meet the oxidizing demand of the system for the oxygen-enriched air gasification scenario and guarantee the gas microturbine's stable operation.

$$AIR_1 = 610.94 \times N_{2split} + 1289.50 \quad (4)$$

where AIR_1 is the airflow amount (kg/h) supplied in the ASU and N_{2split} is the nitrogen amount separated (kg/h).

The technical specifications of the Capstone C200 microturbine considered in the developed model are presented in Table 5.

Table 5. Capstone C200 microturbine datasheet [35].

Parameter	Value
Rating	200 kW
Electrical Efficiency	33%
Net Heat Rate LHV	10.9 MJ/kWh
Exhaust Gas Flow	1.3 kg/s
Compression ratio	4.0

It is recommended to operate downdraft gasifiers above 800 °C to minimize tar production and optimize the carbon conversion rate and syngas production [36]. Therefore, the baseline study adopted a temperature of 850 °C for the reduction zone. Nevertheless, the effect of the variation of the average gasification temperature was also analyzed by a sensitivity study of each system variant. According to Rabou et al. [23], it is only possible to operate a gas microturbine using syngas with an LHV greater than 8 MJ/Nm³, which is then the lowest LHV value considered for power generation in this study. A scheme of the system (gas microturbine, gasifier, and ASU) is shown in Figure S2 (Supplementary Materials).

2.4. Economic Assessment

For the cases that presented technical applicability potential (syngas LHV \geq 8 MJ/Nm³), their economic feasibility was determined based on the net present value (NPV) criterion. The United States dollar was used (USD 1.00 = BRL 5.72 in January 2022). The economic feasibility analysis of the system was complemented with a risk analysis using Monte Carlo simulations performed in Crystal Ball[®] software. The capital expenditure (CAPEX) of the gasification system was estimated according to the Capital Cost Scaling methodology [37], using the reference prices declared by [38,39]. Manufacturers were consulted regarding costs for gas microturbines and ASU.

The assumptions (variables with some degree of uncertainty) adopted during the risk study were:

1. The operation and maintenance costs of the gasification system, excluding biomass cost: range from 3.5 to 5.7% of the gasifier CAPEX [40]. In this study, the mean value (4.6%) was taken as the starting parameter, and during the risk study, the lower and upper limits were subsequently incorporated into the analysis;
2. The operation and maintenance costs of the gas microturbine were estimated at 0.019 USD/kWh from [41], with lower and upper limits of 0.018 and 0.020 USD/kWh during risk analysis, respectively;
3. The electricity price: the reference value for the pre-tax electricity price in the baseline case was 0.1614 USD/kWh (current price). The variation of this parameter was estimated from the local energy price adjustments historical distribution;
4. The biomass (wood pellets) price: the variation range of raw material prices was established from the survey of local prices. The baseline value for the biomass price was 126.37 USD/ton;
5. The net electrical power delivered: a variation of $\pm 15\%$ in the net electrical power delivered due to the operation regime itself was considered;
6. The total capital expenditure investment: it was assumed that a possible short-term local market transformation and fluctuations of $\pm 15\%$ in the international equipment prices could occur.

The minimum acceptable rate of return (MARR) of the system was associated with a weighted average capital cost (WACC) of the renewable energy company under the assumption of a capital structure whose liabilities are 60% equity and 40% debt. The WACC was determined using the capital asset pricing model (CAPM). In this sense, the estimated WACC was 10.32% APY. Once the amounts of investment, income, and expenses were known, the system's cash flow was analyzed. The project's risk of becoming unfeasible

was determined from a Monte Carlo simulation with 100,000.00 trials and a 95% confidence level, considering the lower limit of the economic decision criterion ($NPV \geq 0$).

3. Results

3.1. System Operating with Atmospheric Air as the Gasification Agent

Figure 4 shows the behavior of syngas composition and LHV as ER increases, where oxidation reactions are promoted by increased oxygen availability.

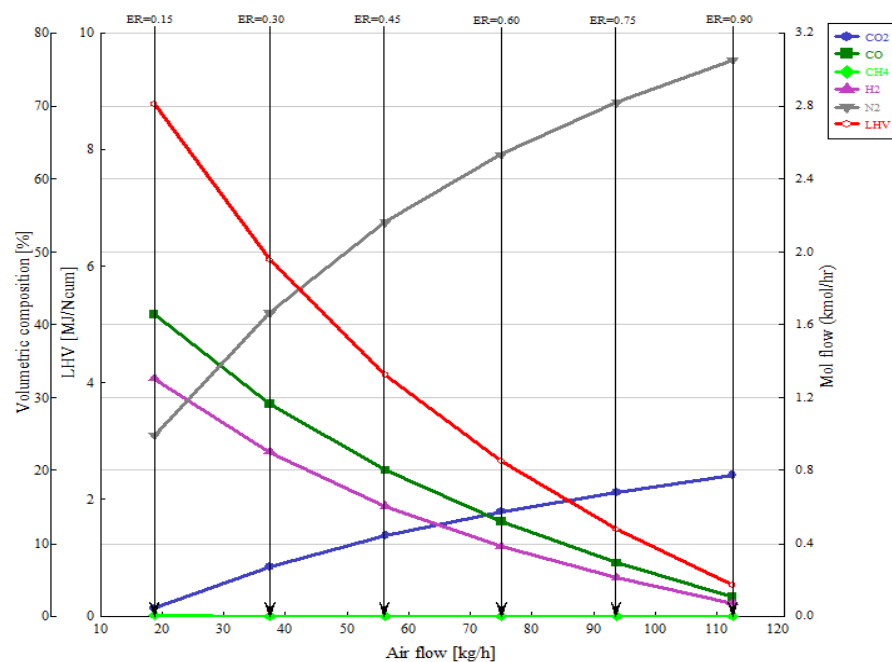


Figure 4. Composition and LHV behavior of the syngas as a function of airflow and ER.

The gasification temperature is particularly relevant to the proposed system. Figure 5 presents the relationship between this variable, the cold gas efficiency (CGE), the syngas LHV, and the yield rate.

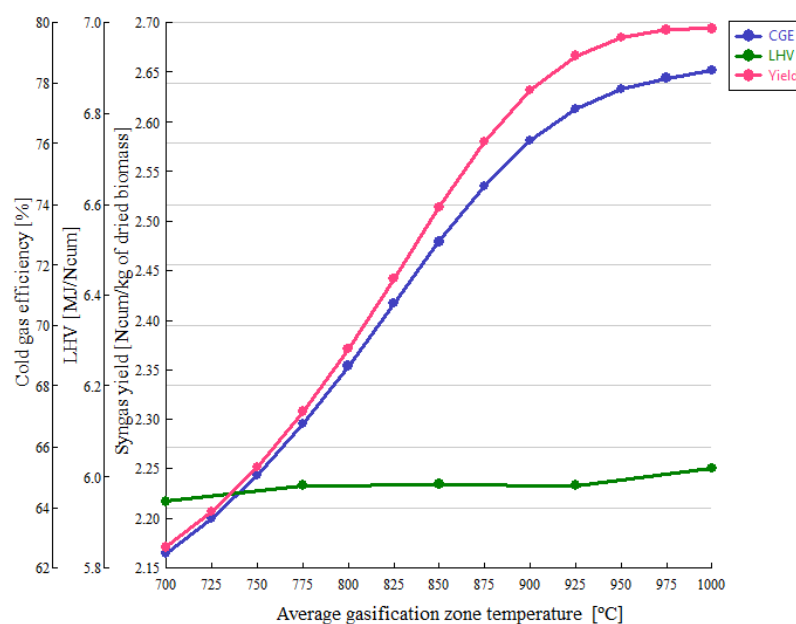


Figure 5. Cold gas efficiency, LHV, and syngas yield as a function of gasification temperature.

In addition to reaching a significant CO content, the syngas obtained from the thermochemical conversion process of wood pellets presented other compounds, such as H_2 and CH_4 , which contribute to the increase in the syngas LHV. Thus, Figure 6 shows the profile of syngas volumetric composition obtained as a function of the gasification temperature.

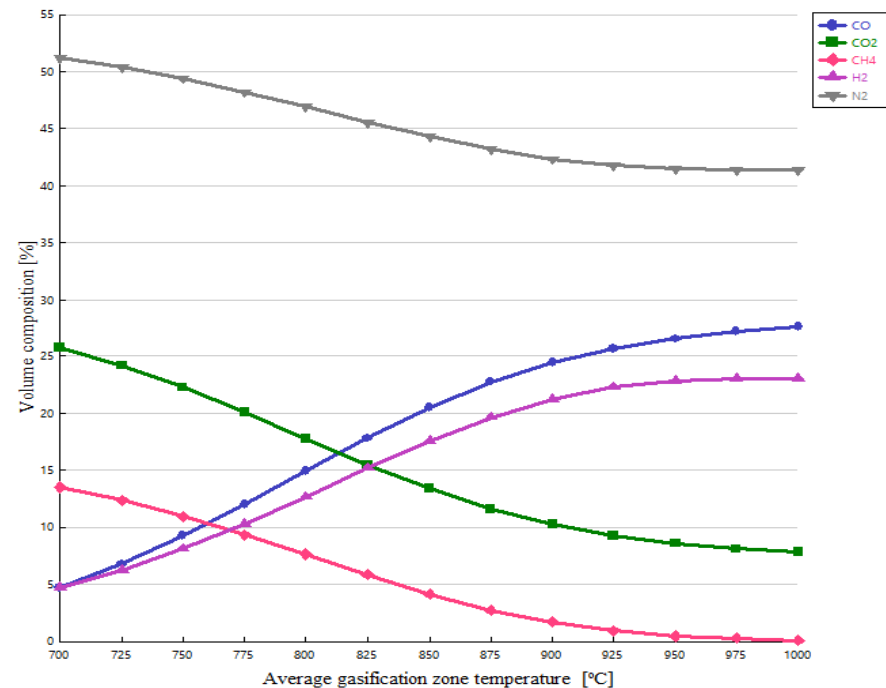


Figure 6. Syngas composition as a function of gasification temperature.

3.2. System Operating with Oxygen-Enriched Air as Gasification Agent

Figure 7 displays the influence of the oxygen concentration in the enriched air on the composition and LHV of syngas, while Figure 8 shows the effects of oxygen concentration in the gasification agent on CGE and syngas yield.

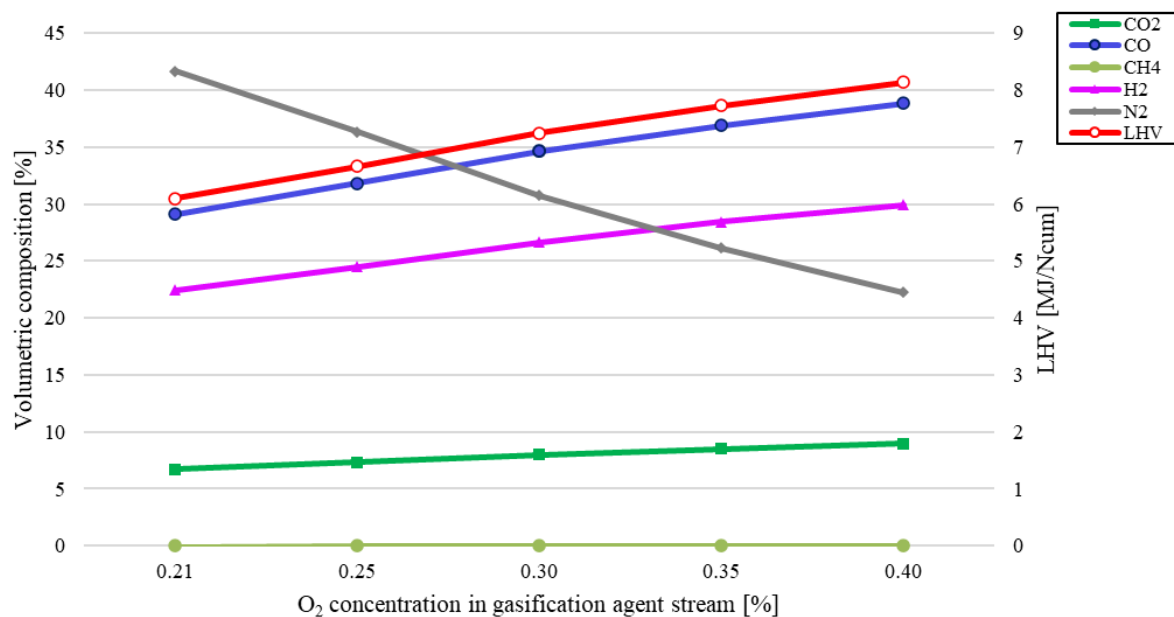


Figure 7. Composition and LHV of syngas as a function of oxygen concentration in the gasification agent.

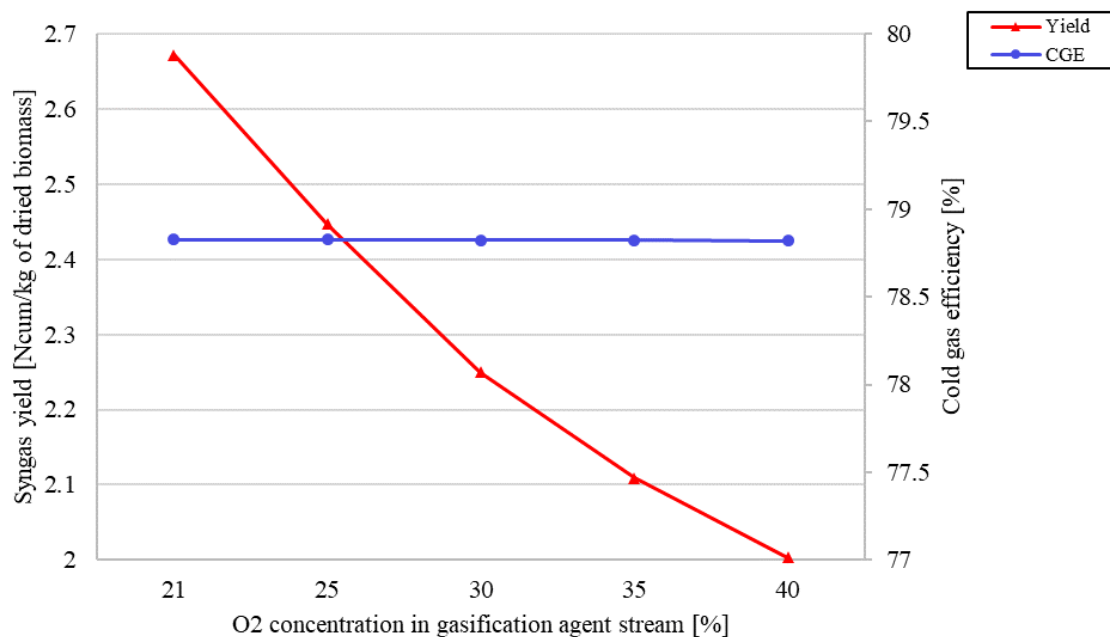


Figure 8. Cold gas efficiency and syngas yield rate as a function of oxygen concentration in the gasification agent.

On the other hand, the behavior of CGE, LHV, and syngas yield for this scenario as a function of the average temperature in the gasification zone is shown in Figure 9. An additional analysis of gasification temperature and LHV syngas is presented in Supplementary Material B (Figure S3).

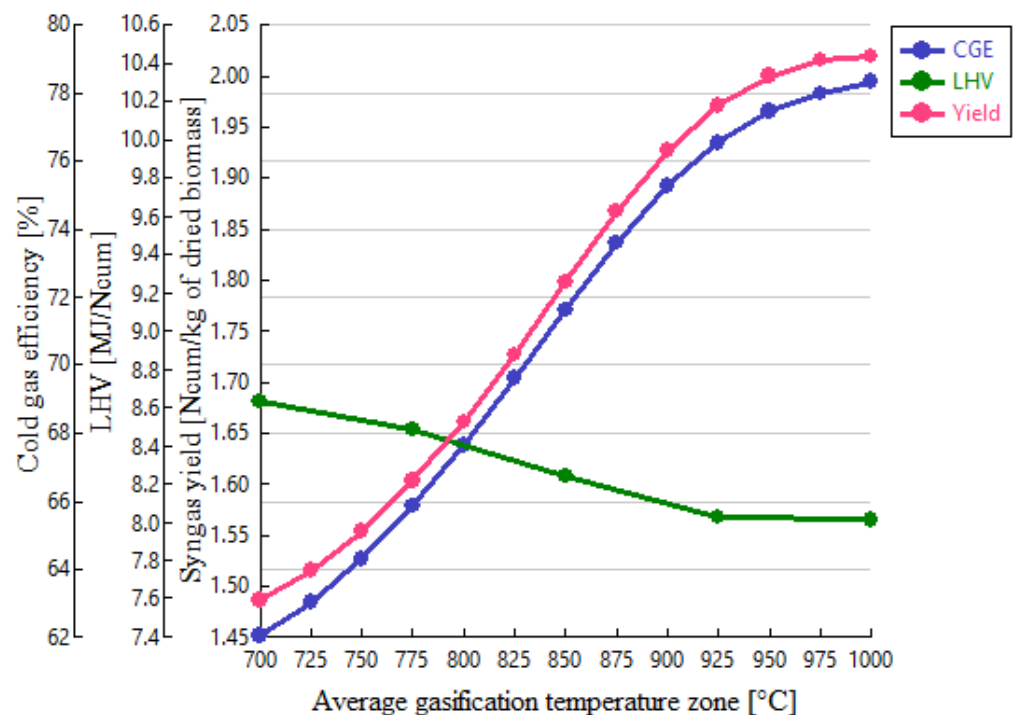


Figure 9. CGE, LHV, and yield rate behavior of syngas as a function of gasification temperature when using oxygen-enriched air ($O_2 = 40\%$).

Due to the partial removal of nitrogen from atmospheric airflow supplied to the gasifier, a significant drop in the content of this compound is observed in the syngas (Figure 10). Figure 11 shows the variation of the power delivered as a function of the

oxygen concentration of the enriched air and the average temperature in the gasification zone; both parameters significantly impact the engine performance.

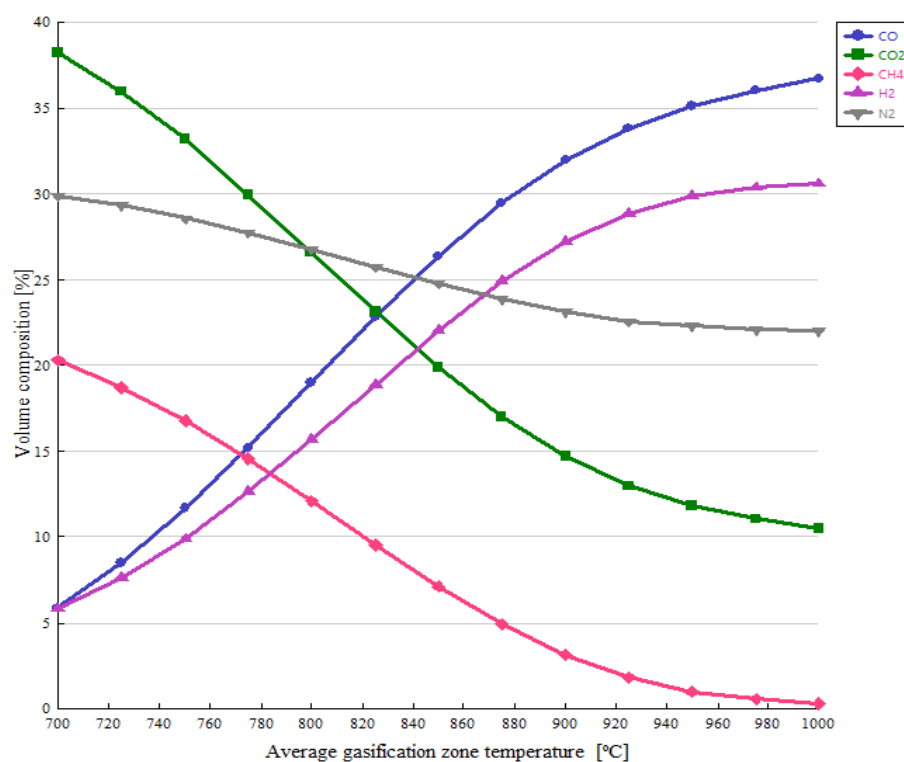


Figure 10. Syngas composition as a function of the gasification temperature when using enriched air ($O_2 = 40\%$).

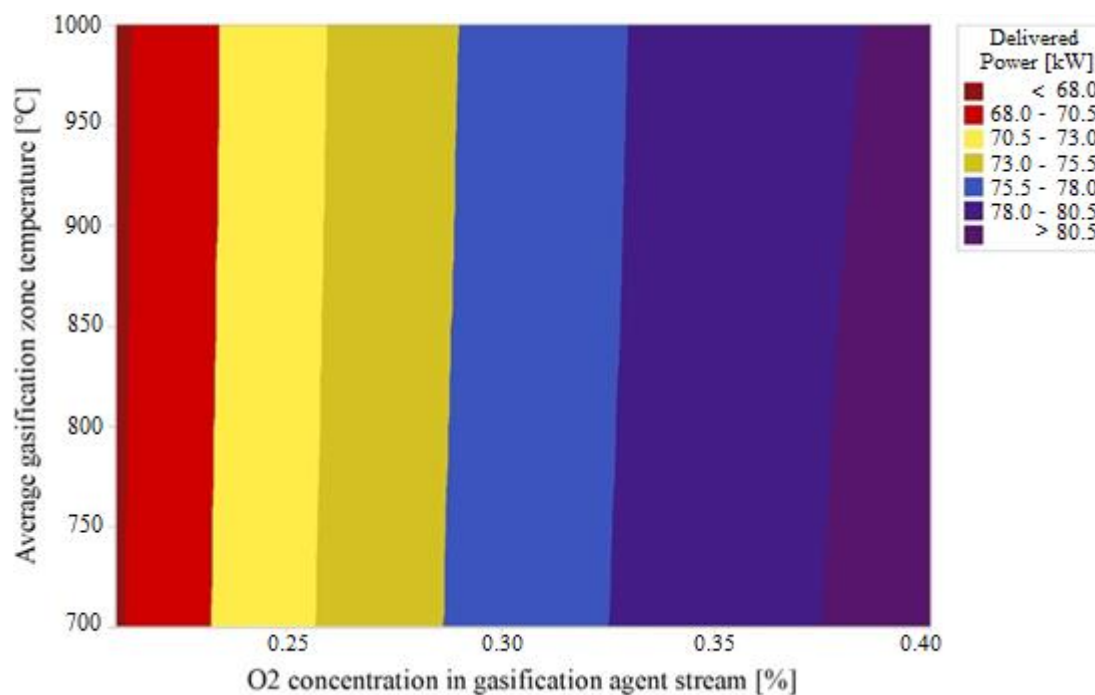


Figure 11. Power delivered by gas microturbine as a function of both the gasification temperature and the oxygen content in enriched air.

The main economic parameters of the proposed system are described in Table 6, where it is possible to observe the investments necessary for its construction in a segregated form.

Table 6. Investment required to construct the downdraft gasifier/gas microturbine system using oxygen-enriched air as the gasification agent.

Feature/Item	Unit of Measure	Magnitude
Electric power	kW	81.35
Availability factor [42]	%	95
Annual energy	kWh/Year	676,994.70
	Investment	
Gas microturbine	USD	347,600.00
Downdraft gasifier (Includes installation)	USD	92,939.61
Air separation unit	USD	8640.00
Canvas gasometer	USD	5001.00
Balance of plant (BOP) [43]	USD	88,107.92
Import taxes	USD	166,303.70
Total	USD	708,592.24

Since the components of the proposed system are not available in the domestic Brazilian market, it will be essential to bear the taxes presented in Table 7 for its importation. The annual revenues, represented by savings in electricity not purchased from the local utility company, are described in Table 8.

Table 7. Taxes on equipment imports in the Brazilian state of Minas Gerais.

Tax	Magnitude
TEC Mercosur	0.00%
IPI	8.00%
PIS	2.10%
COFINS	9.65%
ICMS (Minas Gerais)	18.00%
Total	37.75%

Table 8. Annual revenue from the gas microturbine and downdraft gasifier-based generation system using oxygen-enriched air as a gasification agent.

Parameter	Unit	Magnitude
Electricity price (before tax)	USD/kWh	0.1614
Electricity taxes (Resolution 2550/2019)	%	25.00
Electricity price (After tax)	USD/kWh	0.2017
Annual revenue	USD/Year	136,583.68

The annual operating, maintenance, and fuel (biomass) expenses for the gas microturbine and downdraft gasifier-based generation system are described in Table 9. Other relevant parameters used in the economic assessment are described in Table 10.

Table 9. Annual costs for the gas microturbine and downdraft gasifier-based generation system using oxygen-enriched air as a gasification agent.

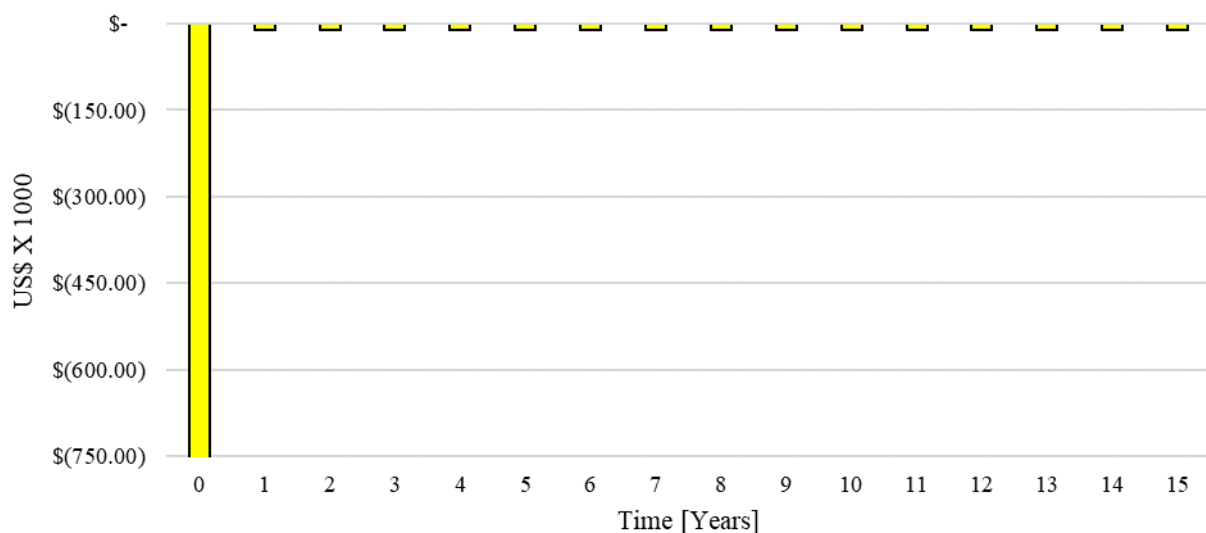
Annual Expenses	Unit	Magnitude
Gas microturbine operation and maintenance (O&M)	USD	12,725.57
Downdraft gasifier operation and maintenance (O&M)	USD	4275.22
Wood pellets	USD	102,956.65
Total	USD	119,957.44

Table 10. Complementary data for the economic feasibility assessment of the gas microturbine and downdraft gasifier-based generation system using oxygen-enriched air as a gasification agent.

Parameter	Unit	Magnitude
Service life	Years	15.00
Brazilian Real/United States Dollar exchange rate	BRL/USD	5.72
Income tax ¹	%	0.00
Depreciation	% APY	10.00
MARR	% APY	10.32
Wood pellets price	USD/ton	126.37

¹ This does not apply because it is a saving, not revenue itself.

From the known data (discount rate, investment segregation, and expenses segregation) and the estimated annual savings resulting from implementing the gas microturbine and downdraft gasifier-based generation system, it was possible to establish the cash flow shown in Figure 12. Note that the initial investment of the host company was USD 708,592.24.

**Figure 12.** Cash flow from the gas microturbine and downdraft gasifier-based generation system using oxygen-enriched air as a gasification agent.

The forecasted statistical distribution for the project NPV and its Max Extreme fit are presented in Figure 13. As can be seen from Figures 14 and 15, the NPV of the venture is highly dependent on the electricity price. The CAPEX, the net electric power delivered by the system, and the biomass cost have marginal effects on economic viability. In addition, the operating and maintenance costs have a negligible impact on the system's economic viability. The benefit/cost ratio of the project is presented in Figure S4 of Supplementary Materials.

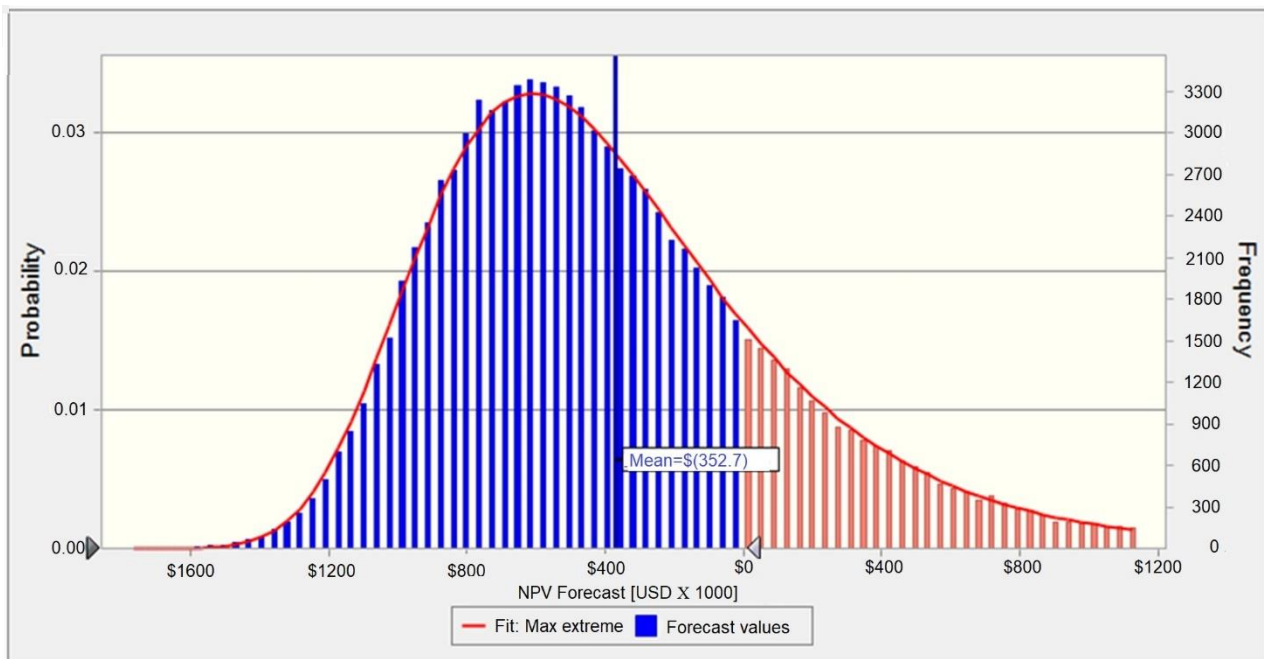


Figure 13. NPV forecast of the gas microturbine and downdraft gasifier-based generation system using oxygen-enriched air as a gasification agent.

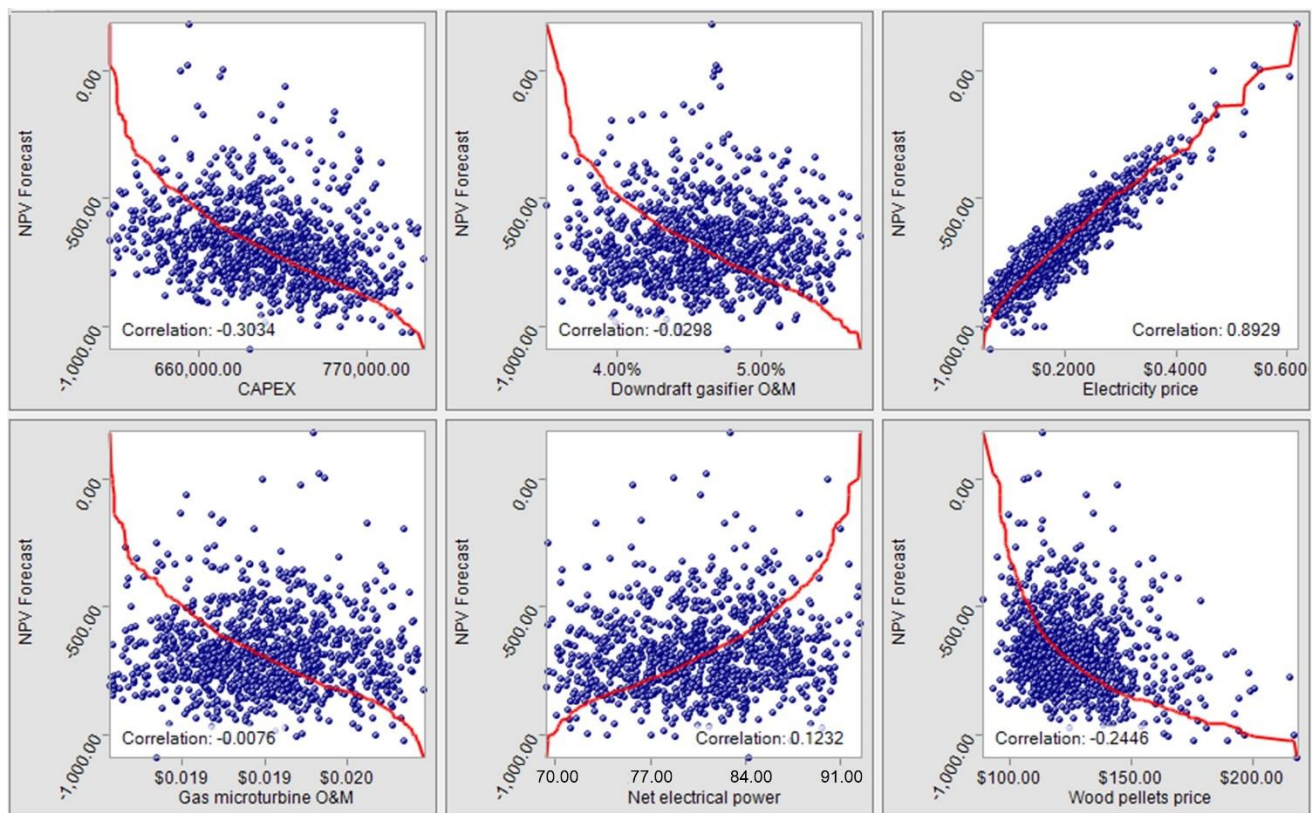


Figure 14. Assumptions scatter plot for the Monte Carlo simulation considering the NPV as a target in the gas microturbine and downdraft gasifier-based generation system.

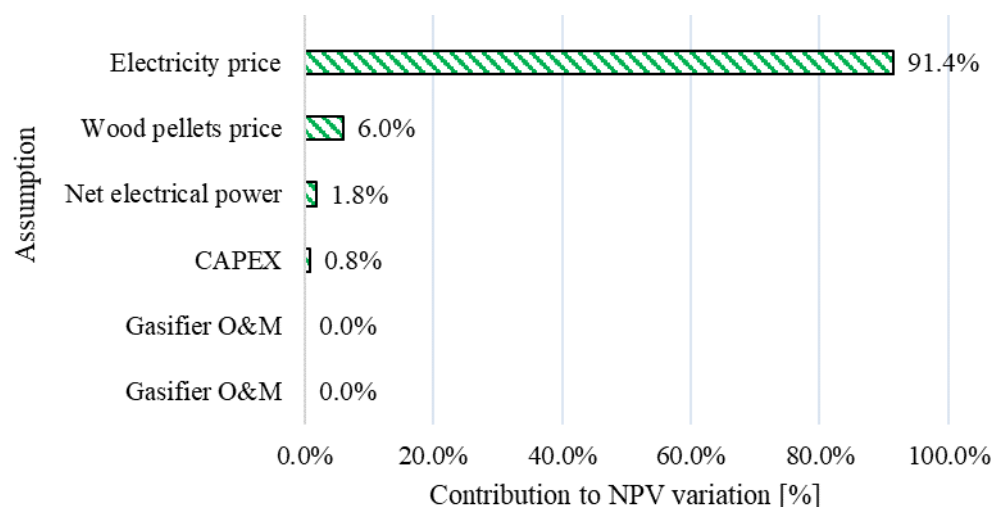


Figure 15. Assumptions contribution to NPV variation in the gas microturbine and downdraft gasifier-based generation system using oxygen-enriched air as a gasification agent.

4. Discussion

Figure 4 shows that the volumetric nitrogen content in the syngas is quite expressive and increases rapidly with the ER increase. The LHV of syngas shows a strong dependence on carbon monoxide and hydrogen fractions; there is a remarkable decline in syngas LHV as the nitrogen fraction increases, as described by Oveisi et al. [44] for the wood chip gasification process.

Figure 5 indicates that the temperature increase favors the syngas yield rate, which is associated with the decomposition and reform of the compounds present in the fuel and, therefore, a greater amount of syngas per mass unit of biomass is produced [45]. This trend agrees with some studies [46–48], where the syngas yield increased as the temperature rose when using air as a gasification agent in the thermochemical conversion of biomass. Regarding syngas LHV, an increasing behavior is observed as the temperature is augmented, which can be explained by temperature influence on the reactions since higher temperatures favor the reforming and thermal cracking reactions of the heavier organic fractions contained in the fuel [49]. Thus, lighter hydrocarbons with lower energy are produced, but combustible gases, such as CO and H₂, increase considerably, leading to higher syngas LHV. Considering the values of syngas LHV obtained in the air gasification scenario, it is possible to conclude that coupling the microturbine to the downdraft gasifier is technically unfeasible. Therefore, the economic analysis of this scenario was not performed.

It is worth noting that the CGE considers only the chemical energy available in the produced gas (chemical contribution of combustible gases, such as H₂, CO, and CH₄, among others) [50]. Therefore, an increasing trend was observed as temperature increased due to the favoring of oxidation reactions. In this way, the content of CO and H₂ in the syngas improved the CGE values, rising from 62% to approximately 78%. On the other hand, Figure 6 showed that the fractions of H₂ and CO increased; this result is associated with the shift and char hydrogenation reactions, since temperatures greater than 700 °C favor the formation of the reactants in equilibrium (Le's Principle Châtelier) [33]. The other reactions that contribute to the formation of H₂ and CO are char gasification and steam methane reforming. However, these last two reactions can be limited after 1000 °C due to the lack of CH₄, the main reactant in reversible reduction reactions [51]. The volumetric fraction of CH₄ decreased as gasification temperature increased, remaining at almost zero for temperatures above 925 °C because methane cracking occurs under these conditions [52].

Figure 7 indicates that when oxygen-enriched air is used as the gasification agent, there is a considerable increase in the syngas LHV as the oxygen concentration in the gasification agent rises. There is also a close relationship between the LHV and the concentration of CO

and H_2 . The depreciation of nitrogen entering the gasifier with the gasification agent leads to a substantial drop in syngas nitrogen content [53].

On the other hand, Figure 8 shows that the volume of syngas produced decreases as the oxygen content in the enriched air increases, a fact already predicted given the partial removal of the nitrogen in the air [54]. CGE remains virtually unchanged with increasing the O_2 content.

Figure 9 shows that the syngas yield rate increased as the temperature increased, but this increment is smaller when compared to the air gasification scenario. Therefore, it is evident that the N_2 content in the oxidant greatly influences the syngas yield [55]. Considering that the N_2 is a chemically inert compound, it will also be part of the syngas composition and, in the oxygen-enriched air gasification case, the N_2 content is lower by the implementation of the ASU unit. The syngas LHV showed a decreasing trend as the temperature increased, where oxygen (in higher concentrations in the gasification agent) and nitrogen in the air favors the formation of CO_2 , and the dilution effect, respectively [56]. Therefore, the content of CH_4 in the syngas decreases, affecting the LHV (8.64 to 8.01 MJ/Nm³). Additionally, a higher oxygen concentration in the gasification agent and the process temperature increase results in a reactor operation near to a combustion regime, contributing to the syngas chemical energy increase and improving the CGE [57].

Figure 10 shows that the fractions of CO and H_2 increased as temperature was augmented, while the fraction of CH_4 was practically null for temperatures higher than 750 °C. These earlier trends can be explained by the chemical reactions in the gasification process. Since the char gasification, steam methane reforming, and Boudouard reactions are endothermic, an increase in temperature will cause the reaction equilibrium to change from reactants to products according to Le Châtelier's Principle [58]. Temperatures greater than 700 °C favor the formation of H_2 and CO (from steam methane reforming reaction), since the CH_4 formed in the char hydrogenation reaction at low temperatures is cracked [59].

Besides the necessity of using higher fuel flow rates in the gas microturbine, due to the low syngas LHV, the presence of CO and H_2 in the combustible gases can lead to combustion instabilities, especially when the hydrogen content surpasses 40%, as reported by Page et al. [24]. These instabilities are related to the anchoring position and structure of the flame inside the combustor. Using an oxygen-enriched gasification agent allows one to obtain the minimum desired LHV (8 MJ/Nm³) with a hydrogen content of around 30%.

In terms of electrical power, when fed with syngas produced in the oxygen-enriched air gasification scenario, the gas microturbine can deliver between 68.53 and 82.71 kW (Figure 11). In the baseline case (ER = 0.30; O_2 = 40%; T = 850 °C), the power produced by the microturbine was 81.24 kW, and its thermal efficiency was 21.35%. The electricity generation system proposed, i.e., the C200 microturbine coupled to the downdraft gasifier using oxygen-enriched air as a gasification agent (including auxiliary systems), has an overall efficiency of 11.82%.

It is worth noting that the economic assessment was conducted from the point of view of a customer whose electrical demand is equal to or superior to the capacity of the proposed generation systems. Hence, with the adoption of this arrangement, the customer will not purchase part of its demand (electricity) from the utility company, which, in economic terms, results in avoided costs. Considering both the discounted rate (WACC = 10.32% APY) and NPV behavior, it is possible to conclude that the investment is economically unviable.

From Figure 13, it could be observed that with an accuracy of 95%, it is possible to state that the probability of experiencing a financial loss (negative NPV) is 79.93%. The mean NPV is USD 352.7, while the NPV probability distribution adjustment standard deviation is USD 234.0. This result is reflected in Figure 15, where it is possible to observe that the project's NPV is highly dependent on the utility's energy tariff (91.4%), while the share of investment CAPEX, the cost of biomass, and the net electrical power delivered by the system have a low impact. Operation and maintenance costs have a negligible effect on the economic viability of this system variant. Therefore, it would be necessary to increase the current price of the electricity purchased from the electrical grid (0.1614 USD/kWh)

by 1.63 times to make the proposed system economically feasible, considering all other constant parameters. The proposed system's resulting installation cost is 8821.53 USD/kW.

5. Conclusions

This work presents the modeling and validation of a gas microturbine and down-draft gasifier system. The results indicate that when using atmospheric air, the system produced syngas with a maximum LHV of 6.10 MJ/Nm³, while with oxygen-enriched air, the LHV ranged from 8.64 to 8.01 MJ/Nm³. Therefore, the syngas LHV obtained using atmospheric air is very low to sustain the gas microturbine operation, while using oxygen-enriched air as the gasification agent, the LHV showed technic feasibility in some cases (LHV > 8.0 MJ/Nm³).

The use of syngas in the gas microturbine leads to decreases in microturbine efficiency from 33% (nominal condition) to 21.35%, while the net power generated ranged between 68.53 and 82.71 kW. It is worth noting that using oxygen-enriched air as the gasification agent results in a system's overall efficiency of 11.82%.

However, from an economic point of view, the system is unfeasible due to the probability of a financial loss (negative NPV) of 79.93%, where biomass prices, electricity delivery, and capital investment play a secondary role in the system's viability. From a hypothesis test, it would be necessary to have very high electricity prices (1.63 times higher than current) to justify the investment, making this system economically impractical nowadays. Therefore, based on the Monte Carlo simulation, it was possible to establish that the electricity price is crucial to enable the proposed system to be economically viable.

Supplementary Materials: The following supporting information can be downloaded at: <https://www.mdpi.com/article/10.3390/pr10112377/s1>, Figure S1: ASU used during downdraft gasifier feeding with oxygen-enriched air; Figure S2: Scheme for oxygen-enriched air gasification scenario; Figure S3: Syngas LHV as a function of both oxygen concentration in enriched air flow and gasification temperature; Figure S4: Benefit/Cost ratio.

Author Contributions: Conceptualization, N.C.H. and Y.C.S.; methodology, O.J.V. and N.C.H.; software, N.C.H. and Y.C.S.; validation, Y.C.S., N.C.H. and E.E.S.L.; formal analysis, D.M.Y.M. and O.J.V.; investigation, E.d.O.P. and E.E.S.L.; resources, J.S.N.H. and E.d.O.P.; data curation, O.H.A.J. and E.E.S.L.; writing—original draft preparation, N.C.H. and Y.C.S.; writing—review and editing, O.J.V., J.S.N.H. and O.H.A.J.; visualization, O.H.A.J.; supervision, E.d.O.P.; project administration, D.M.Y.M.; funding acquisition, E.E.S.L. and O.J.V. All authors have read and agreed to the published version of the manuscript.

Funding: The authors would like to acknowledge the financial support from the Coordination for the Improvement of Higher Education Personnel (CAPES), Brazilian Council for Scientific and Technological Development (CNPq) n° 307223/2017-5, n° 407531/2018-1, n° 311651/2018-6, the PRH of the National Agency for Petroleum, Natural Gas, and Biofuels (PRH-ANP n°51.1), the Research Supporting Foundation of Minas Gerais State (FAPEMIG), Federal University of Itajubá (UNIFEI), and the Federal University of Latin American Integration (UNILA).

Data Availability Statement: Not applicable.

Conflicts of Interest: The authors declare no conflict of interest.

Nomenclature

APY	Annual percentage yield
ASU	Air separation unit
BM	Boston–Mathias alpha function
CAPEX	Capital expenditures
CAPM	Capital asset pricing model
CGE	Cold gas efficiency
COFINS	Contribution to social security financing

DCOALIGT	Non-conventional compounds density
ER	Equivalence ratio
HCOALGEN	Non-conventional compounds enthalpy
IAPWS-95	International association for the properties of water and steam method
ICMS	Tax on the movement of goods and services
IPI	Taxes over industrialized products
LHV	Low heating value
MARR	Minimum acceptable rate of return
NPV	Net present value
ORC	Organic Rankine cycle
PIS	Social integration program contribution
SOFC	Solid oxide fuel cell
TEC	Common external tariff
WACC	Weighted average capital cost
AIR	Air flow for air gasification scenario
AIR ₁	Air flow for oxygen-enriched air gasification scenario
BIOMASS	Biomass flow
ER	Equivalence ratio
N _{2Split}	Removed nitrogen split fraction in ASU

References

1. International Energy Agency. *World Energy Outlook*; International Energy Agency: Paris, France, 2016.
2. Koirala, B.P.; Koliou, E.; Friege, J.; Hakvoort, R.A.; Herder, P.M. Energetic Communities for Community Energy: A Review of Key Issues and Trends Shaping Integrated Community Energy Systems. *Renew. Sustain. Energy Rev.* **2016**, *56*, 722–744. [\[CrossRef\]](#)
3. Castillo Santiago, Y.; Martínez González, A.; Venturini, O.J.; Sphaier, L.A.; Ocampo Batlle, E.A. Energetic and Environmental Assessment of Oil Sludge Use in a Gasifier/Gas Microturbine System. *Energy* **2022**, *244*, 123103. [\[CrossRef\]](#)
4. Marques, T.E.; Castillo Santiago, Y.; Renó, M.L.; Yepes Maya, D.M.; Sphaier, L.A.; Shi, Y.; Ratner, A. Environmental and Energetic Evaluation of Refuse-Derived Fuel Gasification for Electricity Generation. *Processes* **2021**, *9*, 2255. [\[CrossRef\]](#)
5. Benini, E. *Progress in Gas Turbine Performance*, 1st ed.; Benini, E., Ed.; IntechOpen: London, UK, 2013; ISBN 978-953-51-1166-5.
6. Fershalov, A.Y.; Fershalov, Y.Y.; Fershalov, M.Y. Principles of Designing Gas Microturbine Stages. *Energy* **2021**, *218*, 119488. [\[CrossRef\]](#)
7. Henao, N.C.; Lora, E.E.S.; Maya, D.M.Y.; Venturini, O.J.; Franco, E.H.M. Technical Feasibility Study of 200 kW gas Microturbine Coupled to a Dual Fluidized Bed Gasifier. *Biomass Bioenergy* **2019**, *130*, 105369. [\[CrossRef\]](#)
8. Konečná, E.; Teng, S.Y.; Máša, V. New Insights into the Potential of the Gas Microturbine in Microgrids and Industrial Applications. *Renew. Sustain. Energy Rev.* **2020**, *134*, 110078. [\[CrossRef\]](#)
9. Amaro, J.; Mendiburu, A.Z.; de Carvalho, J.A. Thermodynamic Study of Syngas Combustion in Gas Microturbines with Regeneration Composed with Metallic and Ceramic Materials. *Appl. Therm. Eng.* **2019**, *157*, 113285. [\[CrossRef\]](#)
10. Castillo Santiago, Y.; Martínez González, A.; Venturini, O.J.; Yepes Maya, D.M. Assessment of the Energy Recovery Potential of Oil Sludge through Gasification Aiming Electricity Generation. *Energy* **2021**, *215*, 119210. [\[CrossRef\]](#)
11. Martínez González, A.; Silva Lora, E.E.; Escobar Palacio, J.C. Syngas Production from Oil Sludge Gasification and Its Potential Use in Power Generation Systems: An Energy and Exergy Analysis. *Energy* **2019**, *169*, 1175–1190. [\[CrossRef\]](#)
12. Hanchate, N.; Ramani, S.; Mathpati, C.S.; Dalvi, V.H. Biomass Gasification Using Dual Fluidized Bed Gasification Systems: A Review. *J. Clean. Prod.* **2021**, *280*, 123148. [\[CrossRef\]](#)
13. Antolini, D.; Ail, S.S.; Patuzzi, F.; Grigante, M.; Baratieri, M. Experimental Investigations of Air-CO₂ Biomass Gasification in Reversed Downdraft Gasifier. *Fuel* **2019**, *253*, 1473–1481. [\[CrossRef\]](#)
14. Kan, X.; Zhou, D.; Yang, W.; Zhai, X.; Wang, C.-H. An Investigation on Utilization of Biogas and Syngas Produced from Biomass Waste in Premixed Spark Ignition Engine. *Appl. Energy* **2018**, *212*, 210–222. [\[CrossRef\]](#)
15. Liu, L.; Huang, Y.; Cao, J.; Liu, C.; Dong, L.; Xu, L.; Zha, J. Experimental Study of Biomass Gasification with Oxygen-Enriched Air in Fluidized Bed Gasifier. *Sci. Total Environ.* **2018**, *626*, 423–433. [\[CrossRef\]](#) [\[PubMed\]](#)
16. Wang, L.; Du, X.; Chen, J.; Wu, Z. Numerical Study on Characteristics of Biomass Oxygen Enriched Gasification in the New Gasifier on an Experimental Basis. *Renew. Energy* **2021**, *179*, 815–827. [\[CrossRef\]](#)
17. Cui, X.; Song, G.; Yao, A.; Wang, H.; Wang, L.; Xiao, J. Technical and Economic Assessments of a Novel Biomass-to-Synthetic Natural Gas (SNG) Process Integrating O₂-Enriched Air Gasification. *Process Saf. Environ. Prot.* **2021**, *156*, 417–428. [\[CrossRef\]](#)
18. Chuah, C.Y.; Muhammad Anwar, S.N.B.; Weerachanchai, P.; Bae, T.-H.; Goh, K.; Wang, R. Scaling-up Defect-Free Asymmetric Hollow Fiber Membranes to Produce Oxygen-Enriched Gas for Integration into Municipal Solid Waste Gasification Process. *J. Membr. Sci.* **2021**, *640*, 119787. [\[CrossRef\]](#)
19. Sittisun, P.; Tippayawong, N.; Pang, S. Biomass Gasification in a Fixed Bed Downdraft Reactor with Oxygen Enriched Air: A Modified Equilibrium Modeling Study. *Energy Procedia* **2019**, *160*, 317–323. [\[CrossRef\]](#)

20. Cao, Y.; Wang, Q.; Du, J.; Chen, J. Oxygen-Enriched Air Gasification of Biomass Materials for High-Quality Syngas Production. *Energy Convers. Manag.* **2019**, *199*, 111628. [\[CrossRef\]](#)
21. Gu, H.; Tang, Y.; Yao, J.; Chen, F. Study on Biomass Gasification under Various Operating Conditions. *J. Energy Inst.* **2019**, *92*, 1329–1336. [\[CrossRef\]](#)
22. Kolanowski, B.F. *Guide to Microturbines*, 1st ed.; Kolanowski, B.F., Ed.; Fairmont Press: Lilburn, GA, USA, 2004; ISBN 9780824740016.
23. Rabou, L.P.L.M.; Grift, J.M.; Conradie, R.E.; Franssen, S. Micro Gas Turbine Operation with Biomass Producer Gas and Mixtures of Biomass Producer Gas and Natural Gas. *Energy Fuels* **2008**, *22*, 1944–1948. [\[CrossRef\]](#)
24. Page, D.; Shaffer, B.; McDonell, V. Establishing Operating Limits in a Commercial Lean Premixed Combustor Operating on Synthesis Gas Pertaining to Flashback and Blowout. In Proceedings of the ASME Turbo Expo 2012: Turbine Technical Conference and Exposition, Copenhagen, Denmark, 11–15 June 2012; pp. 647–656.
25. Moradi, R.; Marcantonio, V.; Cioccolanti, L.; Bocci, E. Integrating Biomass Gasification with a Steam-Injected Micro Gas Turbine and an Organic Rankine Cycle Unit for Combined Heat and Power Production. *Energy Convers. Manag.* **2020**, *205*, 112464. [\[CrossRef\]](#)
26. Perna, A.; Minutillo, M.; Jannelli, E.; Cigolotti, V.; Nam, S.W.; Yoon, K.J. Performance Assessment of a Hybrid SOFC/MGT Cogeneration Power Plant Fed by Syngas from a Biomass Down-Draft Gasifier. *Appl. Energy* **2018**, *227*, 80–91. [\[CrossRef\]](#)
27. Renzi, M.; Patuzzi, F.; Baratieri, M. Syngas Feed of Micro Gas Turbines with Steam Injection: Effects on Performance, Combustion and Pollutants Formation. *Appl. Energy* **2017**, *206*, 697–707. [\[CrossRef\]](#)
28. Corrêa, P.S.P.; Zhang, J.; Lora, E.E.S.; Andrade, R.V.; de Mello e Pinto, L.R.; Ratner, A. Experimental Study on Applying Biomass-Derived Syngas in a Microturbine. *Appl. Therm. Eng.* **2019**, *146*, 328–337. [\[CrossRef\]](#)
29. Aghaalikhani, A.; Schmid, J.C.; Borello, D.; Fuchs, J.; Benedikt, F.; Rispoli, F.; Henriksen, U.B.; Sárossy, Z.; Cedola, L. Detailed Modelling of Biomass Steam Gasification in a Dual Fluidized Bed Gasifier with Temperature Variation. *Renew. Energy* **2019**, *143*, 703–718. [\[CrossRef\]](#)
30. Basu, P. *Biomass Gasification, Pyrolysis, and Torrefaction: Practical Design and Theory*, 2nd ed.; Basu, P., Ed.; Elsevier Inc.: San Diego, CA, USA, 2013; ISBN 978-0-12-396488-5.
31. Belaissaoui, B.; le Moullec, Y.; Hagi, H.; Favre, E. Energy Efficiency of Oxygen Enriched Air Production Technologies: Cryogeny vs Membranes. *Sep. Purif. Technol.* **2014**, *125*, 142–150. [\[CrossRef\]](#)
32. Zainal, Z.A.; Ali, R.; Lean, C.H.; Seetharamu, K.N. Prediction of Performance of a Downdraft Gasifier Using Equilibrium Modeling for Different Biomass Materials. *Energy Convers. Manag.* **2001**, *42*, 1499–1515. [\[CrossRef\]](#)
33. Han, J.; Liang, Y.; Hu, J.; Qin, L.; Street, J.; Lu, Y.; Yu, F. Modeling Downdraft Biomass Gasification Process by Restricting Chemical Reaction Equilibrium with Aspen Plus. *Energy Convers. Manag.* **2017**, *153*, 641–648. [\[CrossRef\]](#)
34. Capstone. *Capstone MicroTurbine® Fuel Requirements Technical Reference*; Capstone: Chatsworth, CA, USA, 2014.
35. Capstone. *Capstone C200 Microturbine Technical Reference*; Capstone: Los Angeles, CA, USA, 2009.
36. Gagliano, A.; Nocera, F.; Bruno, M.; Cardillo, G. Development of an Equilibrium-Based Model of Gasification of Biomass by Aspen Plus. *Energy Procedia* **2017**, *111*, 1010–1019. [\[CrossRef\]](#)
37. Turner, M.J.; Pinkerton, L.L. *Quality Guidelines for Energy System Studies: Capital Cost Scaling Methodology*; National Energy Technology Laboratory (NETL): Pittsburgh, PA, USA, 2013.
38. Holmgren, K.M. *Investment Cost Estimates for Gasificationbased Biofuel Production Systems*; IVL Swedish Environmental Research Institute: Stockholm, Sweden, 2015.
39. Food and Agriculture Organization (FAO). *Bioenergy and Food Security Rapid Appraisal: User Manual*; FAO: Rome, Italy, 2014.
40. Watson, J.; Zhang, Y.; Si, B.; Chen, W.-T.; de Souza, R. Gasification of Biowaste: A Critical Review and Outlooks. *Renew. Sustain. Energy Rev.* **2018**, *83*, 1–17. [\[CrossRef\]](#)
41. Davidson, K.; Hite, R.; Jones, D.; Howley, A. *A Comprehensive Assessment of Small Combined Heat and Power Technical and Market Potential in California*; California Energy Commission: Sacramento, CA, USA, 2019.
42. Ferrara, M.; Chiang, Y.-M.; Deutch, J.M. Demonstrating Near-Carbon-Free Electricity Generation from Renewables and Storage. *Joule* **2019**, *3*, 2585–2588. [\[CrossRef\]](#)
43. Craig, K.R.; Mann, M.K. *Cost and Performance Analysis of Biomass-Based Integrated Gasification Combined-Cycle (BIGCC) Power Systems*; National Renewable Energy Laboratory (NREL): Golden, CO, USA, 1996.
44. Oveisi, E.; Sokhansanj, S.; Lau, A.; Lim, J.; Bi, X.; Preto, F.; Mui, C. Characterization of Recycled Wood Chips, Syngas Yield, and Tar Formation in an Industrial Updraft Gasifier. *Environments* **2018**, *5*, 84. [\[CrossRef\]](#)
45. Kook, J.W.; Choi, H.M.; Kim, B.H.; Ra, H.W.; Yoon, S.J.; Mun, T.Y.; Kim, J.H.; Kim, Y.K.; Lee, J.G.; Seo, M.W. Gasification and Tar Removal Characteristics of Rice Husk in a Bubbling Fluidized Bed Reactor. *Fuel* **2016**, *181*, 942–950. [\[CrossRef\]](#)
46. Pandey, A.; Bhaskar, T.; Stöcker, M.; Sukumaran, R.K.B.T. *Recent Advances in Thermochemical Conversion of Biomass*; Elsevier: Boston, MA, USA, 2015; ISBN 978-0-444-63289-0.
47. Upadhyay, D.S.; Sakhiya, A.K.; Panchal, K.; Patel, A.H.; Patel, R.N. Effect of Equivalence Ratio on the Performance of the Downdraft Gasifier—An Experimental and Modelling Approach. *Energy* **2019**, *168*, 833–846. [\[CrossRef\]](#)
48. Mun, T.-Y.; Kim, J.-O.; Kim, J.-W.; Kim, J.-S. Influence of Operation Conditions and Additives on the Development of Producer Gas and Tar Reduction in Air Gasification of Construction Woody Wastes Using a Two-Stage Gasifier. *Bioresour. Technol.* **2011**, *102*, 7196–7203. [\[CrossRef\]](#) [\[PubMed\]](#)

49. Martínez González, A.; Lesme Jaén, R.; Silva Lora, E.E. Thermodynamic Assessment of the Integrated Gasification-Power Plant Operating in the Sawmill Industry: An Energy and Exergy Analysis. *Renew. Energy* **2020**, *147*, 1151–1163. [[CrossRef](#)]
50. Martínez González, A.; Silva Lora, E.E.; Escobar Palacio, J.C.; Almazán del Olmo, O.A. Hydrogen Production from Oil Sludge Gasification/Biomass Mixtures and Potential Use in Hydrotreatment Processes. *Int. J. Hydrogen Energy* **2018**, *43*, 7808–7822. [[CrossRef](#)]
51. Lan, W.; Chen, G.; Zhu, X.; Wang, X.; Wang, X.; Xu, B. Research on the Characteristics of Biomass Gasification in a Fluidized Bed. *J. Energy Inst.* **2019**, *92*, 613–620. [[CrossRef](#)]
52. Bizkarra, K.; Barrio, V.L.; Arias, P.L.; Cambra, J.F. Biomass Fast Pyrolysis for Hydrogen Production from Bio-Oil. In *Hydrogen Production Technologies*; Sankir, M., Sankiri, N.D., Eds.; John Wiley & Sons: Hoboken, NJ, USA, 2017; pp. 305–362. ISBN 9781119283676.
53. Sharma, T.; Maya, D.M.Y.; Nascimento, F.R.M.; Shi, Y.; Ratner, A.; Silva Lora, E.E.; Neto, L.J.M.; Palacios, J.C.E.; Andrade, R.V. An Experimental and Theoretical Study of the Gasification of Miscanthus Briquettes in a Double-Stage Downdraft Gasifier: Syngas, Tar, and Biochar Characterization. *Energies* **2018**, *11*, 3225. [[CrossRef](#)]
54. Khosasaeng, T.; Suntivarakorn, R. Effect of Equivalence Ratio on an Efficiency of Single Throat Downdraft Gasifier Using RDF from Municipal Solid Waste. *Energy Procedia* **2017**, *138*, 784–788. [[CrossRef](#)]
55. Kuo, P.C.; Wu, W.; Chen, W.H. Gasification Performances of Raw and Torrefied Biomass in a Downdraft Fixed Bed Gasifier Using Thermodynamic Analysis. *Fuel* **2014**, *117*, 1231–1241. [[CrossRef](#)]
56. Sharma, P.; Gupta, B.; Pandey, M.; Singh Bisen, K.; Baredar, P. Downdraft Biomass Gasification: A Review on Concepts, Designs Analysis, Modelling and Recent Advances. *Mater. Today Proc.* **2021**, *46*, 5333–5341. [[CrossRef](#)]
57. Castillo Santiago, Y.; Pérez, J.F.; Sphaier, L.A. Reaction-Front and Char Characterization from a Palm Kernel Shell—Oil Sludge Mixture under Oxygen Lean Regimes in a Fixed-Bed Gasifier. *Fuel* **2023**, *333*, 126402. [[CrossRef](#)]
58. Liu, Z.; Zhao, C.; Cai, L.; Long, X. Steady State Modelling of Steam-Gasification of Biomass for H₂-Rich Syngas Production. *Energy* **2022**, *238*, 121616. [[CrossRef](#)]
59. Jaffar, M.M.; Nahil, M.A.; Williams, P.T. Synthetic Natural Gas Production from the Three Stage (i) Pyrolysis (Ii) Catalytic Steam Reforming (Iii) Catalytic Hydrogenation of Waste Biomass. *Fuel Process. Technol.* **2020**, *208*, 106515. [[CrossRef](#)]